Caenorhabditis elegans RSD-2 and RSD-6 promote germ cell immortality by maintaining small interfering RNA populations

Aisa Sakaguchi[a,b,1], Peter Sarkies[c,1], Matt Simon[a,d,e,1], Anna-Lisa Doebley[d], Leonard D. Goldstein[c,2], Ashley Hedges[d], Kohta Ikegami[d,3], Stacy M. Alvares[a,f], Liwei Yang[a], Jeannine R. LaRocque[d,4], Julie Hall[d,5], Eric A. Miska[c,1,6], and Shawn Ahmed[a,d,e,1,6]

Departments of [a]Genetics and [d]Biology, [e]Curriculum in Genetics and Molecular Biology, and [f]Seeding Postdoctoral Innovators in Research and Education Postdoctoral Fellowship Program, University of North Carolina, Chapel Hill, NC 27599; [b]Institute for Molecular and Cellular Regulation, Gunma University, Maebashi, Gunma 371-8512, Japan; and [c]The Gurdon Institute, University of Cambridge, Cambridge CB2 1QN, United Kingdom

Edited by Gary Ruvkun, Massachusetts General Hospital, Boston, MA, and approved September 3, 2014 (received for review April 3, 2014)

Germ cells are maintained in a pristine non-aging state as they proliferate over generations. Here, we show that a novel function of the *Caenorhabditis elegans* RNA interference proteins RNAi spreading defective (RSD)-2 and RSD-6 is to promote germ cell immortality at high temperature. *rsd* mutants cultured at high temperatures became progressively sterile and displayed loss of small interfering RNAs (siRNAs) that target spermatogenesis genes, simple repeats, and transposons. Desilencing of spermatogenesis genes occurred in late-generation *rsd* mutants, although defective spermatogenesis was insufficient to explain the majority of sterility. Increased expression of repetitive loci occurred in both germ and somatic cells of late-generation *rsd* mutant adults, suggesting that desilencing of many heterochromatic segments of the genome contributes to sterility. Nuclear RNAi defective (NRDE)-2 promotes nuclear silencing in response to exogenous double-stranded RNA, and our data imply that RSD-2, RSD-6, and NRDE-2 function in a common transgenerational nuclear silencing pathway that responds to endogenous siRNAs. We propose that RSD-2 and RSD-6 promote germ cell immortality at stressful temperatures by maintaining transgenerational epigenetic inheritance of endogenous siRNA populations that promote genome silencing.

germ line | fertility | tudor domain protein

Cellular lifespan is regulated by developmental fate. Somatic cells typically have a limited lifespan of a single generation. In vertebrates, proliferation of somatic cells is governed by an irreversible state of cell cycle arrest that can occur in response to cellular stresses, termed senescence. Senescence is a powerful tumor suppressor mechanism, but it may also contribute to aging. Endogenous stresses have been clearly shown to accumulate with age to cause p53-dependent senescence include telomere attrition and irreparable telomere-associated DNA damage (1, 2). Although distinct sources of endogenous stress accumulate as somatic cells proliferate and induce p16-mediated senescence, natural triggers of this pathway remain unclear (2).

One approach to address forms of stress that could contribute to proliferative aging of somatic cells is to study germ cell immortality. Germ cells have an effectively unlimited proliferative capacity as they are transmitted through the generations (3). Germ cell immortality can be studied by using *Caenorhabditis elegans mortal germline* (*mrt*) mutants that initially possess normal levels of fertility but become progressively sterile. Consistent with telomere attrition as a cause of proliferative aging in humans (4), *mrt* mutants with highly penetrant progressive sterility phenotypes can suffer from progressive telomere shortening as a consequence of defects in telomerase-mediated telomere replication (5, 6), and these mutants typically become sterile at any temperature that they are propagated (7).

We report that the RNAi spreading proteins RNAi spreading defective (RSD)-2 and RSD-6 (8) are required for germ cell immortality at elevated temperatures. RSD-6 is a Tudor domain protein that is homologous to TDRD5 of mammals, which plays a role in spermatogenesis and suppression of transposons (9), whereas RSD-2 does not have any clear mammalian homologs (8). We found that the transgenerational fertility defects of *rsd-2* and *rsd-6* mutants are not restricted to spermatogenesis and are accompanied by desilencing of transposons and other repetitive loci, although transposition does not appear to be the trigger of sterility.

Results

RSD-2 and RSD-6 Promote Germ Cell Immortality at Stressful Temperatures. Many *C. elegans mrt* mutants are temperature sensitive and remain fertile indefinitely at low temperatures but become sterile after growth for multiple generations at the restrictive temperature of 25 °C (5). Of 16 *mrt* mutants that were identified (5), we found that *yp10* and *yp11* were defective in responding to RNA interference, as assessed by feeding *E. coli* expressing double-stranded RNA (dsRNA) triggers (Fig. S1*A*). *yp10* and *yp11*

Significance

Here, we establish a role for small RNAs in promoting transgenerational fertility via an endogenous temperature-sensitive silencing process that is promoted by the RNAi spreading defective (RSD)-2 and RSD-6 proteins, which have been implicated in RNA interference in response to exogenous double-stranded RNA triggers. This process could be broadly relevant to transgenerational maintenance of heterochromatin and is plausibly relevant to regulation of aging of somatic cells as they proliferate.

Author contributions: A.S., P.S., M.S., A.-L.D., L.D.G., A.H., K.I., S.M.A., J.H., and S.A. designed research; A.S., P.S., M.S., A.-L.D., L.D.G., A.H., K.I., S.M.A., L.Y., J.R.L., J.H., and S.A. performed research; P.S. contributed new reagents/analytic tools; A.S., P.S., M.S., A.-L.D., L.D.G., A.H., K.I., S.M.A., L.Y., J.R.L., J.H., E.A.M., and S.A. analyzed data; and A.S., P.S., M.S., A.-L.D., L.D.G., J.R.L., E.A.M., and S.A. wrote the paper.

The authors declare no conflict of interest.

This article is a PNAS Direct Submission.

Data deposition: The data reported in this paper have been deposited in the Gene Expression Omnibus (GEO) database, www.ncbi.nlm.nih.gov/geo (accession no. GSE40460).

[1]A.S., P.S., M.S., E.A.M., and S.A. contributed equally to this work.

[2]Present address: Department of Bioinformatics and Computational Biology, Genentech Inc., South San Francisco, CA 94080.

[3]Present address: Lewis-Sigler Institute for Integrative Genomics and Department of Molecular Biology, Princeton University, Princeton, NJ 08544.

[4]Present address: Department of Human Science, Georgetown University Medical Center, Washington, DC 20057.

[5]Present address: Department of Biology, Lincoln Memorial University, Harrogate, TN 37752.

[6]To whom correspondence may be addressed. Email: shawn@med.unc.edu or eam29@cam.ac.uk.

This article contains supporting information online at www.pnas.org/lookup/suppl/doi:10.1073/pnas.1406131111/-/DCSupplemental.

only became sterile at 25 °C at generation F_4 to F_8 and can be propagated indefinitely at lower temperatures. Outcrosses of *yp10* and *yp11* mutations revealed tight linkage of the exogenous RNAi and Mrt defects. Genetic mapping (Fig. S1*B*), non-complementation tests (Fig. 1*B*), and DNA sequence analysis reveal that *yp10* is an allele of *rsd-2*, whereas *yp11* is an allele of *rsd-6*, two genes with roles in RNAi (Fig. 1*A*) (8). An independent allele of *rsd-6, pk3300*, was reported to become sterile immediately at 25 °C (10), but we found that this phenotype was due to a linked mutation (Fig. S1*B*). Instead, outcrossed *rsd-6* (*pk3300*) lines became progressively sterile at 25 °C at generation F_5 to F_{12}, similar to *rsd-6*(*yp11*) and *rsd-2*(*pk3307*) (sterile at F_5 to F_{12}) (Fig. 1*B*). Thus, mutations in *rsd-2* and *rsd-6* elicit a highly penetrant Mrt phenotype at 25 °C, in which strains display healthy levels of fertility for a number of generations before becoming completely sterile. In contrast, these strains remain completely fertile at the less stressful temperature of 20 °C.

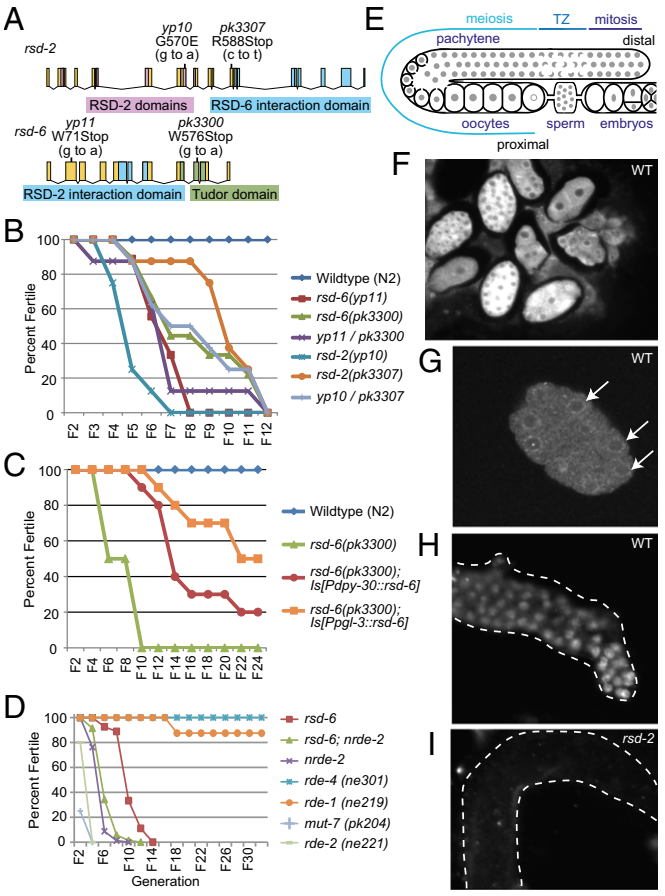

Fig. 1. *rsd-2* and *rsd-6* promote germ cell immortality. (*A* and *B*) *yp10* and *yp11* mutations in *rsd-2* and *rsd-6* (*A*) fail to complement known *rsd-2(pk3307)* or *rsd-6 (pk3300)* mutations for progressive sterility at 25 °C (n = 9 for WT and *rsd-6* mutants, n = 8 for *rsd-2* mutants and for *yp11/pk3300* and *yp10/pk3307* transheterozygotes) (*B*). The RSD-2.a isoform is shown in *A*, but *yp10* and *pk3307* also affect RSD-2.b and .d isoforms (www.wormbase.org). (*C*) A germ-line–specific *pgl-3* promoter-driven *rsd-6* genomic transgene *Is*[*Ppgl-3::rsd-6*] and a ubiquitous *dpy-30* promoter-driven *rsd-6* transgene *Is*[*Pdpy-30::rsd-6*] partially rescued progressive sterility of *rsd-6(pk3300)* at 25 °C (n = 4 for WT and *pk3300*, n = 10 for rescued lines). Incomplete rescue might be due to technical limitations of single-copy *rsd-6* transgenes. (*D*) Lack of an additive fertility defect at 25 °C in *rsd-6 (yp11);* nuclear RNAi defective (*nrde*)*-2(gg95)* double mutants indicates that these genes act in the same pathway to promote germ cell immortality. Deficiency for *rde-4* did not result in progressive sterility at 25 °C, suggesting 26G-RNAs are dispensable for germ cell immortality. (*E*) Model of the *C. elegans* germ line. TZ, transition zone. (*F–I*) Anti–RSD-2 antibody immunofluorescent images assessed by using wide-field (*F*, *H*, and *I*) and confocal (*G*) microscopy. RSD-2 localizes to cytoplasm of wild-type embryos (*F*), where it adopts a perinuclear position (*G*, arrows) and adult germ cell nuclei in wild type (*H*) but not in *rsd-2 (pk3307)* (*I*). The germ line is outlined with dashes lines for *H* and *I*, which are images of the distal germ line that reflect staining throughout the germ line.

RSD-2 and RSD-6 May Function in Germ Cells to Promote Germ Cell Immortality. RSD-6 and RSD-2 form a complex that was previously suggested to promote RNAi spreading from somatic to germ cells (8). However, *rsd-6* and *rsd-2* mutants fail to respond to some somatic RNAi triggers (10) and may simply be deficient for responding to low doses of exogenous dsRNA (8, 11). To test whether *rsd-2* might function in the germ line (Fig. 1*E*), we performed immunofluorescence by using a specific anti–RSD-2 antibody. RSD-2 was found at high levels in the cytoplasm of wild-type embryos (Fig. 1*F* and Fig. S1 *C–E*), where it adopts a perinuclear position (Fig. 1*G*). RSD-2 also localized to nuclei of most wild-type adult germ cells (Fig. 1 *H* and *I*). These results are consistent with previous observations of cytoplasmic and nuclear GFP-tagged RSD-2 in embryos (10), although the specific localization to adult germ cell nuclei observed with our anti–RSD-2 antibody may more precisely reflect endogenous RSD-2. Thus, RSD-2 could function in the germ line and/or in early embryos to promote germ cell immortality.

To test this possibility further, we generated *rsd-6* strains carrying single-copy *rsd-6* transgenes driven by the germ-line–specific *pgl-3* or by the ubiquitous *dpy-30* promoter (12, 13). *Ppgl-3::rsd-6* and *Pdpy-30::rsd-6* transgenes effectively rescued the mortal germ-line defects of *rsd-6*(*pk3300)*, indicating that *rsd-6* functions within germ cells to promote germ cell immortality (Fig. 1*C*). We confirmed this result by creating repetitive extrachromosomal arrays in wild-type animals, which results in "cosuppression" or germ-line–specific silencing of the transgene and the corresponding endogenous gene (14, 15). Cosuppression of *rsd-6* caused a temperature-sensitive Mrt phenotype (Fig. S1 *F* and *G*).

Massive Germ-Line Apoptosis and Chromosome Missegregation Occur in Sterile *rsd* Mutants. Cohorts of completely sterile late-generation *rsd-2(yp10)* (F_6), *rsd-6(yp11)* (F_6), and *rsd-6(pk3300)* (F_8) adults were stained with 4',6-diamidino-2-phenylindole (DAPI) to reveal that many contained germ lines that were either reduced in size or absent (Fig. 2 *A* and *B*). Additionally, unlike wild-type germ lines, a fraction of late-generation *rsd* mutant germ lines were tumorous and showed excessive germ cell proliferation (Fig. 2 *A* and *B*). In contrast, fertile early-generation (F_4) animals maintained at both 20 °C and 25 °C displayed germ line comparable to wild type (Fig. S1*I*). Mutations in the core cell death genes *ced-3* and *ced-4* (16) were used to test whether apoptosis might affect germ-line development in sterile *rsd-2* or *rsd-6* animals. Atrophy and absence of germ-line phenotypes were significantly ameliorated for late-generation *rsd-6(yp11); ced-3* (F_6) and *rsd-6(yp11); ced-4* (F_{10}) double mutants, although the tumorous phenotype persisted (Fig. 2*B*). Thus, germ cell remodeling events promoted by apoptosis occurred in sterile *rsd* hermaphrodites, whereas tumorous germ cell overproliferation occurred independently of apoptosis. In *rsd-6(yp11); ced-3* double mutants, the temperature-sensitive Mrt phenotype of *rsd-6* was not strongly suppressed (Fig. S1*H*), suggesting atrophy of the germ line in late-generation *rsd* mutants is a consequence rather than a cause of germ-line mortality.

Analysis of DAPI-stained oocytes in both early-generation fertile (F_4) and late-generation sterile (F_6–F_8) *rsd-2* or *rsd-6* adults revealed six spots, indicative of a normal karyotype in most of oocytes (Fig. 2 *C* and *D* and Fig. S1*J*). However, some late-generation *rsd* mutant oocytes displayed an increase or decrease in the number of DAPI-positive spots, whereas N2 wild-type siblings propagated for the same number of generations (F_6) did not (Fig. 2 *C* and *D*). Thus, the strong chromosome

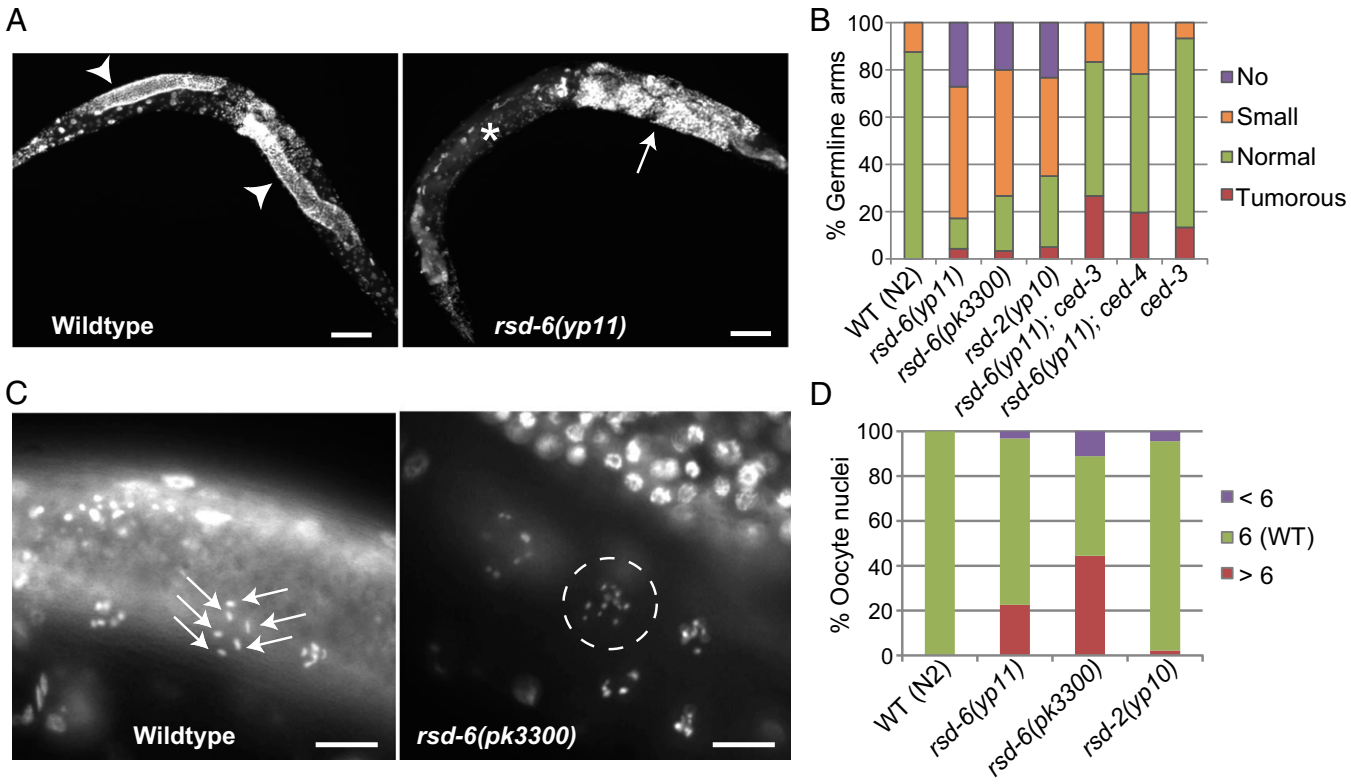

Fig. 2. Germ cell proliferation defects and nondisjunction in late-generation *rsd* mutants. (*A*) DAPI images of wild type reveals normal germ cell proliferation (arrowheads), whereas sterile late-generation (F_6) *rsd-6* mutants display germ cell atrophy (asterisk) or overproliferation (arrow). (*B*) Frequency of germ-line phenotypes in size in sterile late-generation *rsd* mutants and fertile wild-type controls grown at 25 °C (wild type at generation F_6 $n = 40$, *yp11* at F_6 $n = 70$, *pk3300* at F_8 $n = 30$, *yp10* at F_6 $n = 60$, *yp11; ced-3* at F_6 $n = 30$, *yp11; ced-4* at F_{10} $n = 46$, *ced-3* at F_{14} $n = 30$). (*C* and *D*) Images (*C*) and quantification (*D*) of DAPI-positive chromosome spots in oocytes of sterile late-generation *rsd-6* or *rsd-2* adults at 25 °C, and matched fertile wild-type controls (arrows correspond to six chromosomes in diakinesis; dotted circle surrounds a single oocyte nucleus) (wild type at generation F_6 $n = 165$, *yp11* at F_6 $n = 31$, *pk3300* at F_8 $n = 9$, *yp10* at F_6 $n = 45$). (Scale bars: *A*, 100 μm; *C*, 10 μm.)

segregation defects of *rsd-2* and *rsd-6* mutations at sterility are consistent with exacerbation of a previously reported mild chromosome nondisjunction phenotype at high temperature (10). Chromosome missegregation has been noted for other small RNA pathway mutants in *C. elegans* such as CSR-1, an Argonaute protein with roles in promoting chromosome segregation, histone mRNA maturation, and germ-line gene expression (17–19). In addition, RNAi defects lead to desilencing of repetitive DNA in pericentric heterochromatin in *Schizosaccharomyces pombe*, resulting in centromere cohesion defects and chromosome instability (20).

In contrast to late-generation *rsd* mutants (Fig. 2 *C* and *D*), late-generation *mrt* mutants with telomerase defects display consistent decreases in the number of DAPI-positive spots (5, 6). Furthermore, most telomerase mutants are not temperature sensitive and become sterile at all temperatures (5, 6). Thus, defects in telomerase-mediated telomere repeat addition are unlikely to explain the fertility defects of *rsd* mutants.

Small RNAs Targeting Spermatogenesis Genes Are Perturbed in *rsd* Mutants. We hypothesized that RSD-2 and RSD-6 might protect germ cell integrity based on their roles in endogenous RNA silencing pathways. To verify this hypothesis, we fed dsRNA against GFP to strains that carried a germ-line–expressed P*pie-1-gfp* transgene and examined small RNA populations against the *gfp* transgene by RNA sequencing. We found that *rsd-2* mutants are defective for secondary 22G-RNA production or maintenance in the germ line, rather than for primary small interfering RNA (siRNA) biogenesis (Fig. S2 *A*–*F*), consistent with a previous report that RSD-2 and RSD-6 promote secondary siRNA amplification (11).

We next examined small RNA populations from mixed developmental stages of early- (F_2) and late-generation *rsd-2* (F_{10}) and *rsd-6* (F_8) mutant strains grown in parallel at 20 °C and 25 °C. RNA was prepared from late-generation populations that were close to sterility but had very few sterile adults, such that comparable amounts of germ-line tissue would be present in early- and late-generation RNA samples. Deep sequencing of single *rsd-2* or *rsd-6* samples was performed to define consistent molecular changes that occurred at 25 °C (two independent alleles tested per genotype), but did not occur in wild-type controls at 25 °C. We found that 21U-RNAs corresponding to known piRNA (Piwi-interacting RNA) genes (21, 22) were still present and even increased in abundance in late-generation *rsd-2* (F_{10}) and *rsd-6* (F_8) animals (Fig. S2*G*), as were 26G-RNAs, which are also involved in endogenous silencing pathways (Fig. S2*H*) (23). By contrast, 22G-RNAs antisense to protein-coding genes were reduced at a subset of genes after repeated passages (F_{10}) of *rsd-2* animals at 25 °C, and the number of genes showing this reduction was significantly larger in *rsd-2* animals than that in wild-type animals, as revealed by a Q-Q plot where all points would follow the $x = y$ axis if there were no difference between wild type and *rsd-2* (Fig. 3*A*). We identified 481 protein-coding genes that were >16-fold depleted for 22G-RNA reads in late-generation *rsd-2* relative to early-generation *rsd-2* (F_{10}/F_2) grown at 25 °C (Dataset S1). The 22G-RNAs mapping to these genes were also reduced in *rsd-6* late- versus early-generation (F_8/F_2) ($P < 2E{-}16$, Wilcoxon signed rank test) (Fig. S2*I*). Moreover, 22G-RNAs in *rsd-6* late- versus early-generation (F_8/F_2) showed a similar Q-Q plot distribution to *rsd-2* (F_{10}/F_2) (Fig. S2*J*). Genes targeted by these

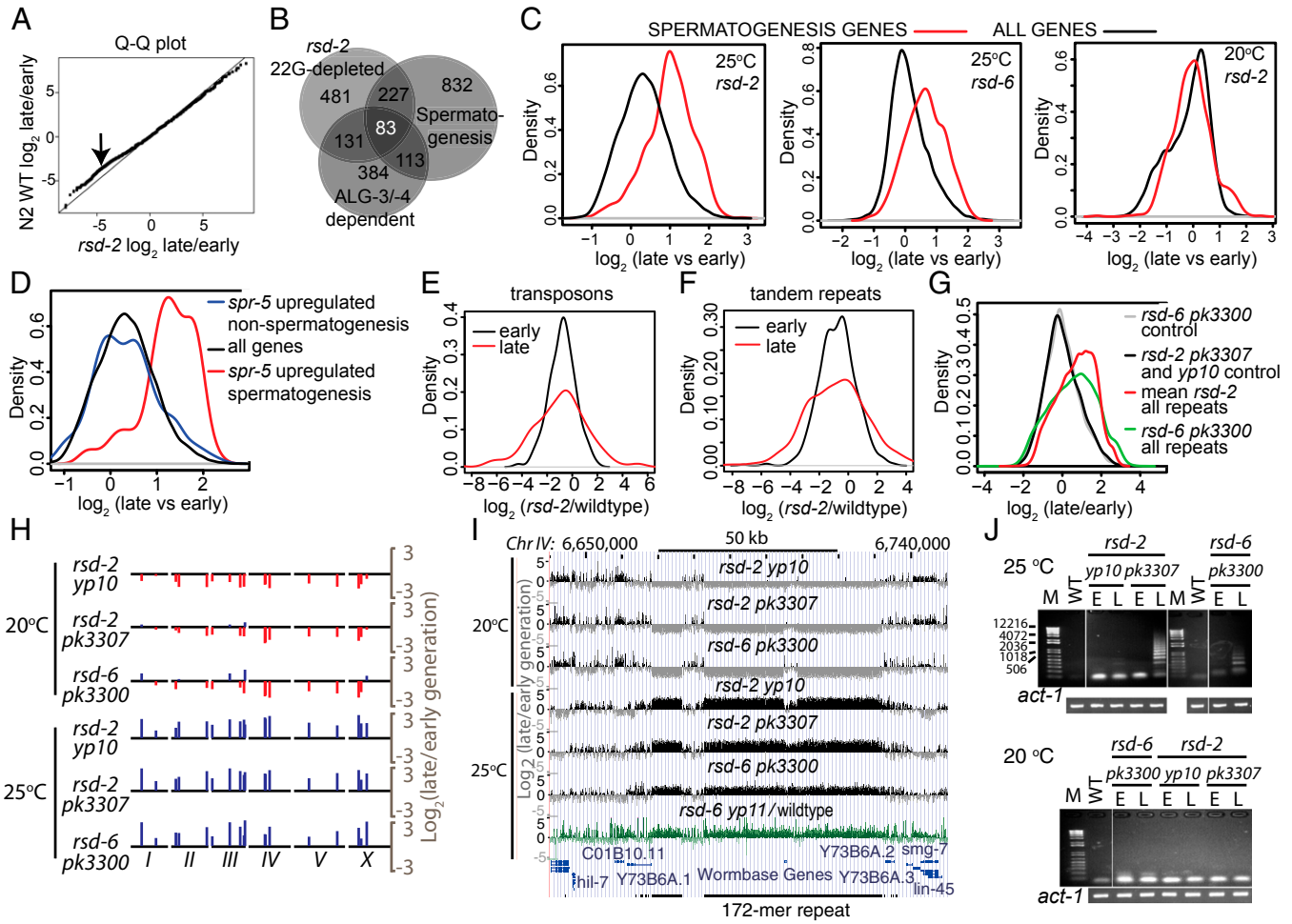

Fig. 3. Gene expression changes in *rsd* mutants associated with loss of small RNAs. (*A*) Q-Q plot to identify differences from normal distribution shows overrepresentation of genes with reduced antisense small RNAs at 25 °C in late- versus early-generation *rsd-2* mutants compared with late- versus early-generation wild type. Arrow indicates deflection from the expected $y = x$ line distribution. (*B*) Overlap of 22G-RNA–depleted genes in late-generation *rsd-2* strains at 25 °C with spermatogenesis and ALG-3/-4 regulated genes (24). The total number of genes in each set including subsets is shown inside the relevant section. (*C*) Tiling array analysis shows up-regulation of spermatogenesis genes in late- versus early-generation *rsd* strains at 25 °C but not at 20 °C. Zero indicates no change in expression. Shift to the right indicates increased expression. Density reflects the number of genes at a specific expression level relative to other segments. (*D*) Tiling array analysis indicates spermatogenesis genes that are up-regulated by *spr-5* show higher expression in late- versus early-generation *rsd-2* mutants at 25 °C but nonspermatogenesis genes that are up-regulated by *spr-5* does not. (*E* and *F*) RNA sequencing analysis shows wider spread of 22G-RNA reads, normalized to total library size, mapping with up to two mismatches to transposons (*E*) or tandem repeats (*F*) in late-generation *rsd-2* strains at 25 °C. (*G*) Expression of tandem repeats increases in late-generation *rsd* mutants, compared with control sequences of the same length drawn randomly from nonrepetitive regions of the genome at 25 °C. (*H*) Expression of the 19 longest tandem repeat tracts in the *C. elegans* genome in late- versus early-generation *rsd* mutants analyzed by tiling arrays. (*I*) Tiling array data from UCSC genome browser reveals up-regulation of a 172-mer repeat tract in late- versus early-generation *rsd* strains grown at 25 °C but not at 20 °C, and also in late-generation *rsd-6* versus late-generation wild-type RNA at 25 °C. (*J*) RT-PCR analysis confirms results shown in *I*. E, early generation. L, late generation. M, size marker. *act-1* PCR is shown as loading control. For RNA sequencing, tiling array, and RT-PCR, *yp10* at generation F_{12}, *pk3307* at F_{10}, *pk3300* at F_8, *yp11* at F_8, and wild type grown for the same number of generations in each experiment were used for late-generation samples, and animals at F_2 were used for early-generation samples for all of the strains tested.

depleted 22G-RNAs overlapped strongly with genes downstream of ALG-3/-4-dependent 26G-RNAs (P = 1E−16, Fisher's exact test) (Fig. 3*B*), which have been shown to target spermatogenesis genes (24) (see below). Consistently, the set of RSD-2–dependent genes also overlapped strongly with spermatogenesis genes (25) (P < 2E−16, Fisher's exact test) (Fig. 3*B*). We compared these genes to a set of 248 genes that show reduced 22G-RNAs in *rsd-2* mutants grown at 20 °C relative to wild type (11). There was a statistically significant overlap between the two sets of genes (P < 1E−3, Fisher's exact test); however, none of the spermatogenesis genes affected in *rsd-2* mutants at 25 °C were also affected at 20 °C (Fig. S2*K*), thus the progressive reduction in small RNAs mapping to spermatogenesis genes in *rsd* mutants only occurs at higher temperatures.

The overlap between genes with RSD-2–dependent small RNAs and genes with ALG-3/-4–dependent small RNAs was intriguing because ALG-3/-4, in conjunction with the Argonaute CSR-1, is required for fertility by maintaining high levels of spermatogenesis gene expression (26). Indeed, RSD-2–dependent genes overlapped more strongly with genes that are up-regulated by ALG-3/-4 than genes down-regulated by ALG-3/-4 (odds ratio 2; Fig. S2*L*) (27). We therefore tested whether loss of RSD-2 function results in altered spermatogenesis gene expression. Systematic examination of the expression of 760 spermatogenesis genes (25) using tiling microarrays across the *C. elegans* genome demonstrated strong up-regulation in late-generation versus early-generation 25 °C *rsd-2* (F_{10}/F_2) and *rsd-6* (F_8/F_2) animals (for both *rsd-2* and *rsd-6*, P < 2E−16, Mann–Whitney unpaired test) (Fig. 3*C* and Dataset S2).

This up-regulation was not seen at 20 °C (*rsd-2*, $P < 2E{-}16$; *rsd-6*, $P < 2E{-}16$, Wilcoxon signed rank test) (Fig. 3*C*), and down-regulation of spermatogenesis genes occurred infrequently. Thus, in contrast to ALG-3/-4 and CSR-1, RSD-2/-6 are required to repress the expression of spermatogenesis genes, implying that the cause of transgenerational sterility in *rsd-2* mutants is distinct. In support of this hypothesis, we found that fertility was rarely restored when mating sterile *rsd-6* hermaphrodites with wild-type males (n = 0/98, 2/132, 2/36, 1/48, and 1/40 sterile *rsd-6* hermaphrodites mated with wild-type males gave rise to progeny in five independent trials). Thus, the transgenerational sterility of *rsd* mutants primarily arises from more widespread germ-line dysfunction than defects in spermatogenesis alone.

Increased expression of spermatogenesis genes in *rsd-2/-6* mutants is reminiscent of the phenotype of the *spr-5* histone H3 lysine 4 demethylase mutant, which shows varying levels of transgenerational sterility (27, 28). However, the spermatogenesis genes targeted by *rsd-2* are not exactly the same as those targeted by SPR-5 (Dataset S2); moreover, there was no up-regulation of non-spermatogenesis genes targeted by *spr-5* (27) in late-generation (F_{10}) *rsd-2* mutants (Fig. 3*D*). This result implies that although RSD-2, RSD-6, and SPR-5 repress spermatogenesis gene expression, SPR-5 regulates a distinct repertoire of targets. Thus, the transgenerational sterility phenotype of *rsd-2/-6* mutants is distinct from those of *alg-3/-4*, *csr-1*, and *spr-5* mutants (29).

Desilencing of Repetitive Loci in Stressed Late-Generation *rsd* Mutants. In addition to targeting 22G-RNAs, vertebrate and *Drosophila* Tudor domain proteins are known to target repetitive regions of the genome such as transposons (9, 30–34). We therefore mapped 22G-RNAs in *rsd* mutants against these repetitive loci. In late-generation (F_{10}) *rsd-2* animals grown at 25 °C, we found significantly wider distribution of differences for 22G-RNAs mapping against transposons (Fig. 3*E*) and tandem repeats (Fig. 3*F*) such that some showed increased 22G-RNA reads and some showed strongly reduced 22G-RNA reads (both $P < 2E{-}16$, Kolmogorov–Smirnov test). We also found that *rsd-2* and *rsd-6* showed highly comparable changes at individual transposon loci (Fig. S3). Moreover, similarly to *rsd-2*, the wider distribution of differences was seen for 22G-RNA reads against tandem repeats and transposons in 25 °C *rsd-6* late-generation (F_8) animals (tandem repeats $P < 0.05$, transposons $P < 2E{-}16$, Kolmogorov–Smirnov test) (Fig. S4 *A* and *B*). We also mapped 22G-RNAs from previously published sequencing data of *rsd-2* mutants grown at 20 °C (11) to transposons and tandem repeats. Although 22G-RNA reads against transposons showed little difference from wild type (Fig. S4*C*) and although a small subset of repeats showed reduced reads (Fig. S4*D*) at 20 °C, there was no evidence of the widespread dysfunction that was seen at 25 °C. Thus, RSD-2 and RSD-6 proteins promote accumulation of 22G-RNAs targeting repetitive regions of the genome at the stressful temperature of 25 °C, an activity that is consistent with a silencing defect that promotes sterility in *rsd* mutants, as discussed below. Consistently, genome-wide, we saw a dramatic increase in the expression of repetitive repeat regions compared with control regions of the genome in both *rsd-2* (F_{10}) and *rsd-6* (F_8) late-generation animals at 25 °C (Fig. 3 *G* and *H* and Fig. S4*E*), but not at 20 °C (Fig. 3*H* and Fig. S4*F*) ($P < 2E{-}16$, Wilcoxon signed rank test). The up-regulated loci included transposons (Fig. S5*A*) and short direct tandem repeat tract loci, composed of 25- to 180-mer repeat tract and total lengths up to 50 kb (Fig. 3*I* and Fig. S5 *B* and *C*), as confirmed by RT-PCR analysis of *rsd* samples (Fig. 3*J* and Fig. S5*D*). Changes in the expression of repetitive elements was associated with altered small RNAs as simple repeats showing both increased and decreased 22G-RNAs in *rsd-2* mutants were more strongly up-regulated than all simple repeats (Fig. S5*E*) (both $P < 0.05$, Wilcoxon unpaired test). Thus, widespread dysfunction in small RNAs from repetitive loci in *rsd-2* mutants is associated with failure to control expression of these elements. Interestingly, although transposons with both increased and decreased 22G-RNAs were up-regulated in *rsd-2* mutants, all transposons also showed up-regulation (Fig. S5*F*), thus suggesting that there might be a more complex relationship between 22G-RNAs and transposon expression in *rsd-2* mutants.

Because the microarray analysis was performed by using RNA from mixed stages of development, we examined the cellular localization of repetitive RNA expression in adults and early embryos using RNA fluorescence in situ hybridization (FISH). We detected RNA from independent tandem repeat sequences in embryos for all strains examined at 25 °C (Fig. 4 *A–C*, *G–I*, and *M–R* and Fig. S6 *P–R*) and also at 20 °C for wild type, including both antisense and sense probes of *CeRep59* (Fig. S6 *S–U*). We did not detect tandem repeat RNA in the adult germ line or somatic cells of wild-type animals (Fig. 4 *G–I* and *P–R*, and Fig. S6 *P–U*) or in control midgeneration (F_6) *rsd-6* mutants at 25 °C (Fig. 4 *M–O*), suggesting that tandem repeats are silenced there. However, we saw a strong signal for tandem repeat probes in both the germ line and somatic cells of late-generation (F_8) *rsd-2* and *rsd-6* mutants grown at 25 °C (Fig. 4 *A–F* and *J–I*, and Fig. S6 *A–C* and *J–O*). Control RNA FISH probes for repetitive loci that express 26S ribosomal RNA were detected at high levels in the germ line of all strains examined, and this signal did not change in late-generation (F_8) *rsd-6* animals (Fig. S6 *D–I*). Thus, RNA from repetitive regions accumulates in both somatic and germ cells of *rsd* mutants concomitantly with the onset of sterility.

Expression of RNA from both strands of repetitive loci during embryogenesis could promote production of siRNAs that silence repeats in the germ line and soma of wild-type adults (Fig. 4 *G–I* and *P–R*, and Fig. S6 *P–U*). Although it was shown that the 26G-RNA class of primary siRNAs that target endogenous loci for silencing are generated during embryogenesis by RDE-4 (35), we found that deficiency for *rde-4* did not result in progressive sterility at 25 °C (Fig. 1*D* and Fig. S1*K*). Thus, although deficiency for *rde-4* has been shown to cause reduced fertility at 25 °C (36), we conclude that *rde-4* is not necessary for long-term transgenerational maintenance of fertility at 25 °C. Therefore, 26G-RNAs are dispensable for germ cell immortality. Note that deficiency for some genes required for 26G-RNA biogenesis results in immediate sterility at 25 °C (*eri-1* and *rrf-3*) (35, 37–39), and freshly outcrossed mutations that disrupt secondary siRNA production, *rde-2* and *mut-7* (40, 41), also result in rapid sterility at 25 °C (Fig. 1*D*) (n = 20 strains propagated per genotype). Deficiency for an additional RNAi gene, *rde-1*, which is required for responding to exogenous dsRNAs (42), resulted in negligible effects on transgenerational fertility (Fig. 1*D*) (n = 8 strains propagated).

Because repetitive elements including transposon loci were desilenced in *rsd-2* and *rsd-6* animals, increased levels of transposition might account for the progressive sterility phenotype. Transposition of a few DNA transposons can be scored based on established excision assays (42), but these tests represent a limited analysis of the diversity of RNA and DNA transposons present in the *C. elegans* genome. We therefore used unbiased tests that would detect increased activity for any transposon and obtained three independent lines of evidence that increased levels of transposition are unlikely to occur in late-generation *rsd* mutants (Fig. S5 *G–K*).

RSD-6 Acts via Small RNA-Mediated Transcriptional Silencing. Because RSD-2 localized to nuclei of adult germ cells (Fig. 1*H*) where tandem repeats were ectopically expressed in late-generation *rsd-2* and *rsd-6* mutants grown at 25 °C (Fig. 4 and Fig. S6), we hypothesize that RSD-2 and RSD-6 promote germ cell immortality in nuclei of adult germ cells. It was reported that three genes that promote RNAi-mediated silencing at genomic loci within nuclei are required for germ cell immortality (43). Mutation of one of these nuclear RNAi genes, *nrde-2*, results in sterility if propagated at 25 °C, similar to *rsd-2* and *rsd-6* (Fig. 1*D*), whereas deficiency for *nrde-1* and *nrde-4* compromises germ cell immortality at all

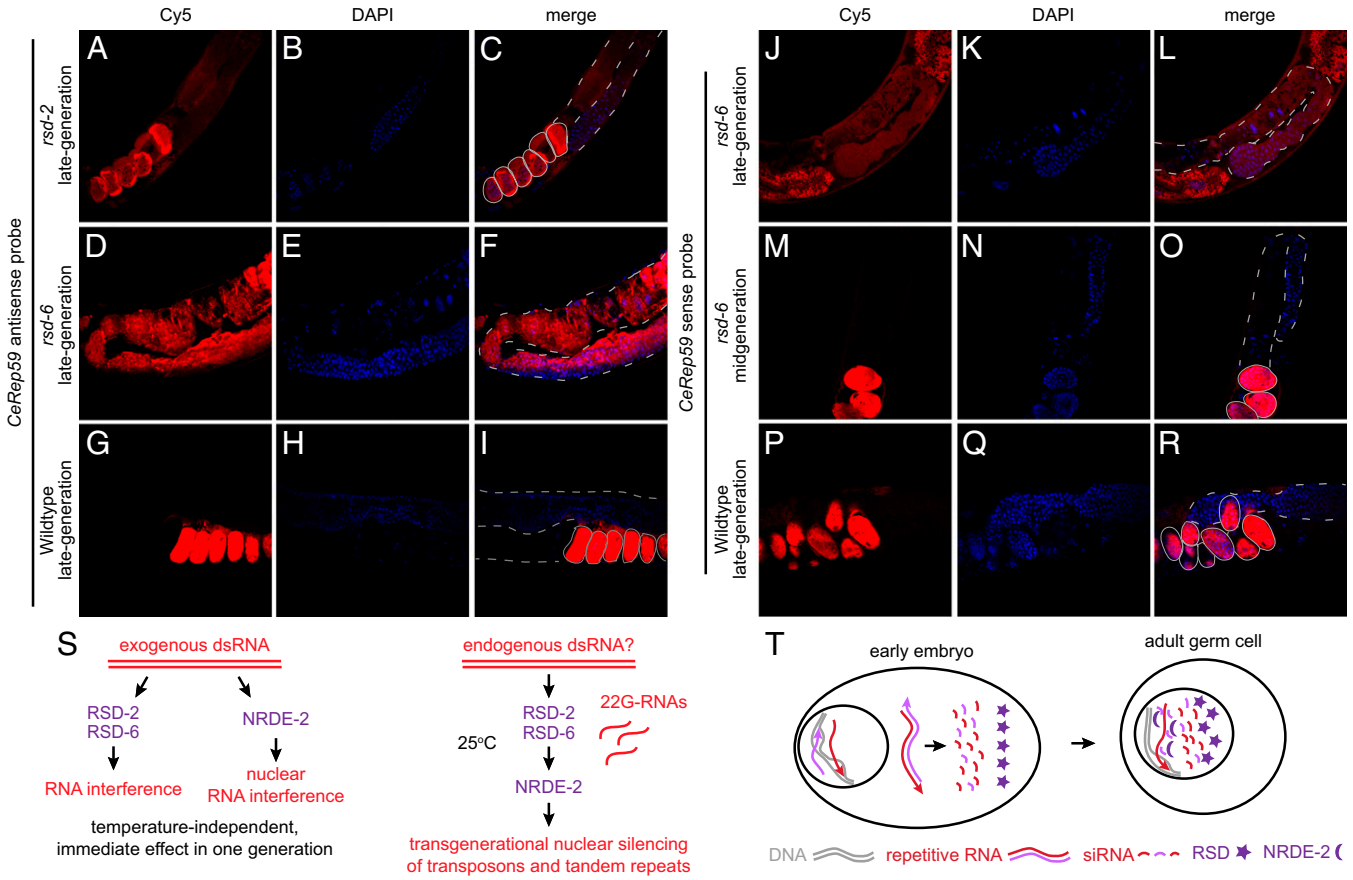

Fig. 4. Germ-line and somatic expression of tandem repeats in late-generation *rsd* mutants. (*A–R*) Confocal images of Cy5-labeled RNA FISH probes (*A, D, G, J, M,* and *P*), DAPI-stained nuclei of the corresponding images (*B, E, H, K, N,* and *Q*), and merged images containing Cy5 and DAPI signals (*C, F, I, L, O,* and *R*) for animals derived from strains grown at 25 °C. RNA FISH probes reveal expression of *CeRep59* antisense tandem repeat (*A–I*) or *CeRep59* sense tandem repeat (*J–R*) in late-generation (F_8) *rsd-2(pk3307)* (*A–C*), *rsd-6(yp11)* (*D–F* and *J–L*) or control midgeneration (F_6) *rsd-6* (*M–O*), and control wild-type (*G–I* and *P–R*) two-day-old adults. All images were taken under the same condition. The germ line is outlined with white dashed line, and embryo is outlined with white solid line for merge images. (*S* and *T*) Models of RSD-2/-6 and NRDE-2 function in transgenerational silencing. RSD-2/-6 and NRDE-2 function via independent RNA silencing pathways with immediate effects in response to exogenous dsRNA (*S, Left*). However, they function in a common transgenerational nuclear silencing pathway that responds to endogenous siRNAs and is revealed only at high temperature (*S, Right*). Expression of forward (purple) and reverse (red) strands of RNA from repetitive loci occurs in early embryos (*T,* left cell), which may lead to siRNA production in the cytoplasm. In adult germ cells, RSD proteins translocate to the nucleus (*T,* right cell), where they may act with NRDE-2 to facilitate a temperature-sensitive process that promotes transgenerational siRNA-mediated silencing of repetitive loci.

temperatures (43). To determine how *nrde-2* and *rsd* mutations interact in the context of germ cell immortality, we constructed *rsd-6(yp11); nrde-2(gg95)* double mutants, which displayed a transgenerational lifespan (6.66 ± 0.18 generations) that was slightly longer than that of *nrde-2* mutants (5.72 ± 0.14 generations) (Fig. 1*D* and Table S1). Lack of an additive fertility defect in *rsd-6; nrde-2* double mutants, compared with single mutant controls, indicates that these genes act in the same pathway to promote germ cell immortality. Consistently, late-generation (F_{12}) sterile *nrde-2* mutant adults grown at 25 °C expressed high levels of repeat RNA in both germ and somatic cells relative to fertile, early-generation (F_2) controls, and this result was comparable with *rsd-6* mutants (Fig. S7).

Discussion

We demonstrate that *rsd-2* and *rsd-6* are required for germ cell immortality at 25 °C, where strains display robust fertility for many generations and then yield a highly penetrant sterile phenotype. This mortal germ-line phenotype implies gradual accumulation of a heritable defect. Our data argue that perturbed transgenerational maintenance of 22G secondary siRNA populations occurs as *rsd* mutants are propagated at 25 °C (Fig. 3 *E* and *F* and Fig. S4 *A* and *B*), resulting in a genome-wide failure of epigenetic silencing and infertility.

C. elegans harbors both prosilencing and antisilencing secondary siRNA systems, where prosilencing 22G-RNAs associate with WAGO-class Argonaute proteins and antisilencing 22G-RNAs associate with ALG-3/-4 and CSR-1 Argonaute proteins. Both these pathways have been implicated in transgenerational sterility phenotypes (26, 44). Conine et al. reported that heterozygosity for *alg-3/-4* or *csr-1* mutations in males can elicit a temperature-sensitive mortal germ-line phenotype, apparent only at 25 °C (26). This phenotype was accompanied by transgenerational depletion of antisilencing 22G-RNA populations associated with CSR-1 and by reduced expression of spermatogenesis genes. Further, late-generation sterility of *alg-3/-4* or *csr-1* heterozygotes was caused by a highly penetrant spermatogenesis defect that was frequently and strongly rescued by wild-type sperm (26). Our finding that *rsd* mutants lose 22G-RNAs against spermatogenesis genes is reminiscent of this effect; however, *rsd* mutants show transgenerational increase in expression of spermatogenesis genes rather than the reduced expression presumed to underlie the phenotype of *csr-1* heterozygosity. Moreover, the fertility of *rsd* mutants cannot be rescued by wild-type sperm. Our data therefore suggest that RSD-2 and RSD-6 do not act in the same pathway as CSR-1/ALG-3/-4 to maintain spermatogenesis gene expression. However, *spr-5* mutants were

recently reported to display a fully penetrant temperature-sensitive progressive sterility phenotype similar to that of *rsd-2* and *rsd-6* (29), and it is possible that the transgenerational sterility phenotypes of these mutants could result from related/overlapping defects in 22G-RNA–directed histone methylation that promote transgenerational silencing of spermatogenesis genes.

Our study suggests that a key function of RSD-2, RSD-6, and NRDE-2 is to promote germ cell immortality via a common transgenerational endogenous small RNA-mediated nuclear silencing process (Figs. 1*D* and 4*S*). Because *rsd-2*/*-6* and *nrde-2* mutants only became sterile at 25 °C, RSD-6 and RSD-2 may function in conjunction with NRDE-2 at the crux of an intrinsically temperature-sensitive process that is essential for germ cell immortality, possibly involving maintenance of prosilencing endogenous 22G-RNAs populations that promote maintenance of heterochromatin (Fig. 4*T*). Such a model is reminiscent of small RNA-mediated heterochromatin silencing in yeast, *Drosophila*, and plants (45).

Despite the involvement of the nuclear RNAi pathway in silencing repetitive sequences, we detected both forward and reverse strands of tandem repeat sequences in the cytoplasm in wild-type embryos (Fig. 4 and Fig. S6). Thus, bursts of transcription from repetitive loci during embryogenesis may generate both primary and secondary siRNAs against these sequences. These data suggest a developmentally regulated mechanism of siRNA production that promotes transgenerational maintenance of prosilencing siRNA populations associated with heterochromatin. Interestingly, RSD-2 was cytoplasmic in embryos, whereas in adults, we observed RSD-2 in the nuclei of germ cells. This observation suggests that RSD-2 could couple cytoplasmic siRNA production with maintenance of NRDE-2–dependent nuclear silencing in the adult germ line and soma (Figs. 1 *F–H* and 4 and Figs. S6 and S7), thus acting to link cytoplasmic and nuclear RNAi pathways. Alternatively, expression of repetitive loci during embryogenesis may represent a developmentally conserved stage of reprogramming of silent chromatin that is separable from the function of RSD-2/RSD-6 in siRNA maintenance at repetitive loci, which could be restricted to nuclei of adult germ cells (right cell of Fig. 4*T*), consistent with RSD-2 localization (Fig. 1*H*).

Our data imply that RSD-2 and RSD-6 promote transgenerational maintenance of siRNA populations that repress expression of repetitive loci such as transposons and tandem repeats (Fig. 4 *S* and *T*). Despite increased expression of transposons, we found no evidence for transposition in late-generation *rsd* mutants (Fig. S5 *G–K*). Lack of a marked increase in transposon-induced mutations may be because there are several layers of defense against transposons, so increased expression of transposon RNA could occur without significant increases in transposition. However, even without increased transposition, increased expression of repetitive regions of the genome including transposons or tandem repeats or associated effects on chromosome architecture may contribute to the transgenerational fertility defect of *rsd* mutants.

Overall, our data indicate that spermatogenesis genes and repetitive segments of the genome are targeted by 22G small RNAs, and that these small RNA populations are disrupted in late-generation *rsd* mutants. However, it is not clear whether increased expression of repeats or spermatogenesis genes, or misexpression of other genomic loci, is sufficient to cause the fertility defects of *rsd* mutants. Thus, the causal connection between small RNA dysfunction and germ-line mortality remains unsolved, and our model represents one of several possible scenarios based on our observations.

One goal of studying germ cell immortality in *C. elegans* is to create models for forms of stress that may be relevant to aging of mammalian somatic cells as they proliferate (50–100 cell divisions). Although the overproliferation and underproliferation phenotypes of sterile *rsd* adult germ cells may appear to be effects of an opposite nature (Fig. 2), proliferative aging of mammalian somatic cells has potentially analogous consequences, where age-related stress can trigger senescence or apoptosis but can also lead to inappropriate overproliferation in the context of tumor development. Our data suggest that a malleable siRNA-based repeat silencing system in germ cells, which may be subject to stochastic, genetic, or epigenetic effects in human populations, could explain some of the transgenerational variation in the penetrance of aging-related disorders.

Materials and Methods

Strains. Unless noted otherwise, all strains were cultured at 20 °C on Nematode Growth Medium plates seeded with *E. coli* OP50 (46). Strains used include Bristol N2 wild type, *dpy-5(e61) I, mut-2(r459) I, rde-2(ne221) I, unc-13(e450) I, unc-13(e51) I, rsd-6(yp11) I, rsd-6(pk3300) I, daf-8(m85ts) I, unc-29(e193) I,* EG4322 *ttTi5605 II (Mos1); unc-119(ed3) III, nrde-2(gg95) II, rde-4(ne301) III, sma-2(e502) III, sma-3(e491) III, unc-32(e189) III, mut-7(pk204) III, ced-4(n1162) III, unc-30(e191) IV, ced-3(n717) IV, unc-26(e205) IV, rsd-2(yp10) IV, rsd-2 (pk3307) IV, dpy-4(e1166) IV, rde-1(ne219) V, dpy-11(e224) V, unc-58(e665) X.*

RNAi mutants *mut-2* and *rsd-6* were outcrossed by using *unc-13* as a marker. RNAi mutant *rde-4* was outcrossed by using *unc-32* as a marker. *rsd-2* and *rde-1* were outcrossed by using *unc-30* and *dpy-11* as markers, respectively.

Mutator assays were performed at 25 °C with late-generation *unc-58* single mutant and *rsd-6; unc-58* or *rsd-2; unc-58* or *mut-2; unc-58* double mutants as described (47).

Germ-Line Mortality Assay and Brood Size Count. Worms were assessed for the mortal germ-line phenotype by using the assay described (5).

Mrt assays were performed for Fig. 1*D* by using *rde-4* animals that were freshly outcrossed at 20 °C. These assays were initiated with six F_4 L1 larvae from nonstarved F_2 plates, and six L1 larvae were transferred to fresh plates once a week (every two generations). For data shown in Fig. 1*D*, the "F_2" generation refers the six 20 °C F_4 L1 larvae placed at 25 °C.

Feeding-RNAi Assay. Feeding RNAi plates harboring host bacteria HT115(DE3) engineered to express *pop-1*, *par-6*, or *pos-1* dsRNA were prepared from the Ahringer RNAi library (48). L4 larvae were placed onto freshly prepared feeding RNAi plates with dsRNA induced by 1 mM IPTG (isopropyl-β-D(-)-thiogalactopyranoside) and were transferred animals every 24 h (49). Assays were performed at 20 °C.

Gene Silencing via Cosuppression. A fragment from 2 kb upstream to 1 kb downstream of *rsd-6* gene including the first and second exons was amplified from N2 wild-type genomic DNA for the cosuppression experiment. The amplified fragment was injected into N2 wild-type animals with pCes1943 [*rol-6(su1006)*] marker, and animals with transgenes were distinguished by the Roller phenotype of *su1006*.

DAPI Staining. DAPI staining was performed as described (5). L4 larvae were selected from sibling plates, and sterile adults were single as late L4s, observed 24 h later for confirmed sterility, and then stained. The stained animals were observed by Nikon Eclipse E800 microscope.

RSD-2 Immunofluorescence. Adult hermaphrodites raised at 20 °C were dissected in M9 buffer and flash frozen on dry ice before fixation for 20 min in methanol at –20 °C. After washing in PBS supplemented with 0.1% Tween-20 (PBST), a rabbit polyclonal antibody against amino acids 581–730 of RSD-2 (F52G2.2) (SDIX) at a 1/3,000 dilution in PBST was used to immunostain overnight at 4 °C in a humid chamber. Secondary antibody staining was performed by using an Alexa-Fluor 488-coupled mouse anti-rabbit, for 1 h at 37 °C. Slides were visualized by using a Zeiss (Fig. 1 *F*, *H*, and *I* and Fig. S1 *C–E*) or Olympus Upright Confocal microscope (Fig. 1*G*). Staining was also carried out in parallel on *rsd-2(pk3307)* animals and showed no reactivity of the antibody with embryos, germ line, or oocytes.

RNA Preparation and cDNA Synthesis. RNA for tiling arrays, RT-PCR, and RNA sequencing was prepared at each generation. Mixed staged animals were collected with M9 buffer, and total RNA was purified by a guanidinium thiocyanate-phenol-chloroform (TRIzol) extraction method (50). First-strand cDNA was synthesized by using Super Script II or III Reverse Transcriptase (Invitrogen). Second-strand cDNA for tiling array was synthesized by using Second Strand Buffer (Invitrogen), *E. coli* DNA ligase (NEB), *E. coli* DNA polymerase I (Promega), and T4 DNA polymerase (NEB). Synthesized cDNA

were fragmented by sonication for tiling arrays. Animals harvested for RNA preparation were predominantly adults from the indicated generation, and embryos and larvae of the following generation.

Tiling Arrays. Tiling microarrays were performed as described (51). The detection platform was Roche NimbleGen Custom 2.1 M Tiling arrays, with 50-mer probes, tiled every 50 bp for the WS170 (ce4) genome build, providing even and almost gap-free coverage across the whole *C. elegans* genome. Samples were amplified by using ligation-mediated PCR as described (52). Late-generation mutant samples were labeled with Cy5, and their input reference late-generation wild type or early-generation mutant with Cy3 following the methods was described (52). Single microarrays were performed for each early- versus late- or late- versus late-generation experiment, using RNA samples from independent alleles of *rsd-2* and *rsd-6*, which play similar roles in RNAi and germ cell immortality, and whose gene products have been shown to physically interact (8).

Microarray Data Analysis. Unless otherwise stated, each mutant allele was treated separately and the difference between late and early generation was calculated. One array, for *rsd-6(yp11)*, had to be discarded because of abnormal background and was not used for further analysis. To test for expression changes in expression of genes identified as expressed during spermatogenesis (25), data normalized for gene bodies was analyzed by using custom scripts in R (25). Statistical testing for spermatogenesis gene expression changes was performed by using the entire set of spermatogenesis genes as a sample so that a paired test could be carried out between changes at 20 °C and at 25 °C, and an unpaired test between changes in spermatogenesis genes and all genes. For *rsd-2*, this statistical test was carried out for both alleles separately giving qualitatively similar data. Plots in Fig. S2*J* were drawn with the mean of both alleles for *rsd-2* and for *pk3300* for *rsd-6*. Repeat expression was analyzed by mapping probes to either repetitive regions downloaded from the University of California, Santa Cruz (UCSC) genome browser website (http://genome.ucsc.edu), or to control regions randomly selected from each chromosome to have the same distribution of lengths as the repeats on the same chromosome. Statistical testing for repeat up-regulation was performed as for gene expression changes. Nonparametric methods were used in both cases to avoid assumptions of normality.

Analysis of Copy Number Changes. *Z* scores comparing comparative genome hybridization intensity from early- and late-generation *rsd-6* animals grown at 25 °C were interrogated for regions annotated as transposons or tandem repeats by using the ce6 genome (WS190) annotation. Each set was compared with control regions randomly selected with the same length distribution as the test set as described for microarray data analysis. Statistical testing for increased copy number analysis was performed by using nonparametric methods. This method was successful in identifying increased copy number of transposons in late-generation mutants lacking *prg-1* (44).

Small RNA Sequencing Analysis. The 5′ independent small RNA sequencing was performed as described (12), using one repeat for each time-point of N2 WT, *rsd-2*, and *rsd-6* at 25 °C. Custom Perl scripts were used to select different small RNA species from the library. To map small RNA sequences to genes, reads were aligned to the *C. elegans* ce6 genome by using Bowtie, Version 0.12.7, requiring perfect matches. Data were normalized to the total number of aligned reads, and 1 was added to the number of reads mapping to each gene to avoid division by zero errors. To map 22G-RNA sequences to transposons and tandem repeats, direct alignment to the transposon consensus sequences, downloaded from Repbase (Ver 17.05) or repeats obtained from the ce6 genome (WS190) annotations downloaded from UCSC as above, was performed by using Bowtie, allowing up to two mismatches and reporting only the best match. Uncollapsed fasta files were used for these alignments to compensate for the problem of multiple identical matches. Data were normalized to the total library size, and 1 was added to the number of reads mapping to each feature to avoid division by zero errors. To analyze data from *rsd-2* mutants grown at 20 °C (11), Fasta files were downloaded from the Gene Expression Omnibus and uncollapsed by using a custom Perl script before aligning to transposons or tandem repeats as above. Analysis of data was carried out by using the R statistical package.

RT-PCR Analysis. Total RNA was isolated as described above. RT-PCR was accomplished by using the Anchor T primer (ATACCCGCTTAATTTTTTTTTTTT) with SuperScript III First Strand Synthesis System (Invitrogen). The resulting cDNA was then normalized by using serial cDNA dilutions with *act-1* specific primers with Ex Taq polymerase (TaKaRa), a 64 °C annealing temperature and 30 PCR cycles. cDNA concentrations were normalized based on ethidium bromide fluorescence of samples separated on 1% agarose gels. Tandem repeats were then analyzed by using PCR amplification with a 65 °C annealing temperature and 28 PCR cycles. PCR primers used were as follows:

act-1 Fwd: GATATGGAGAAGATCTGGCATCA;
act-1 Rev: GGGCAAGAGCGGTGATT;
TanRepI Fwd: CGATGCTCTTTGTAGACAAATCA;
TanRepI Rev: GCACCCAATATTTAGAGAACAGAAG;
TanRepIII Fwd: CATAGGGCATCGAAAAGCAC;
TanRepIII Rev: GAAAATCATCAATTTCTGGAGGC;
TanRepIV Fwd: GAACTTTTGAAACATGTCCCAAC;
TanRepIV Rev: GCCATGCGTTTGTACATATCATAC.

Genetic Mapping and Complementation Tests of *sma-3* Lines. Each of the five *sma* mutations was outcrossed away from the original *rsd* mutations to analyze what might have caused the Small or Dumpy phenotype. To determine whether the Small/Dumpy phenotype occurred in the same gene for all five mutations, *sma; unc-3* double mutants were created and crosses with F_1 $sma^{-/+}$ males that were generated from crosses of $sma^{-/-}$ hermaphrodites with wild-type males. Sma animals were observed in non-Unc cross progeny for all combinations of the five independent *sma* alleles, indicated that they failed to complement one another, and are likely to be alleles of the same gene.

We used a SNP mapping approach (53) to genetically map the *sma* mutations and found that they were located on chromosome *III*, between −7 and +1.55 map units. Mutations in three genes within this genetic interval, *sma*-2, *sma-3*, and *daf-4*, are known to cause small body size (54). Heterozygous *sma-2(e502)*/+ or *sma-3(e491)*/+ males were crossed with each *sma; unc-3* double mutant lines and progeny were scored for the Small phenotype. All F_1 cross progeny sired by *sma-2(e502)*/+ males were wild type while a proportion of F_1 cross-progeny sired by *sma-3(e491)*/+ males exhibited a Small phenotype, indicating failure to complement *sma-3*. Primers were generated to amplify the entire genomic region of *sma-3*, and PCR products created with these primers were sequenced in both directions for each allele and for wild type to clearly show that each *sma* mutation occurred as a consequence of the same single nucleotide insertion. Primers used to amplify the *sma*-3 coding region were AATTCAGGTGGTTGCGAGAAG and TTTCCGCTCAGTTTACCCAC. Sequencing primers were AATTCAGGTGGTTGCGAGAAG, ACTTTGACCAGTGGCATGTTC, CGTTGAGCTTCCACTAGACTGC, AACTTTCATAAGCGCGTCGAG, TTGAGCCTCCTTCCTCTTAGTC, TTTCCGCTCAGTTTACCCAC and AAGCTTCGAATCAGCAATTTTCA.

RNA FISH. DNA oligonucleotide probes coupled with a 5′ Cy5 fluorophore were used to detect repetitive element expression. The four probes used in this study were as follows:

tttctgaaggcagtaattct, *CeRep59* on chromosome *I* (located at 4281435–4294595 nt);

agaattactgccttcagaaa, antisense *CeRep59* on chromosome *I*;

caactgaatccagctcctca, chromosome *V* tandem repeat (located at 8699155–8702766 nt); and

gcttaagttcagcgggtaat, 26S rRNA.

Probes were diluted in RNase free TE buffer immediately before use to produce a working 25 mM stock.

The strains used for RNA FISH experiments were *rsd-6(yp11)*, *rsd-2(pk3307)*, and N2 Bristol wild type. Mixed stage animals were washed off from nonstarved plates into microcentrifuge tubes, then washed once in M9 buffer and three times in 1 mL of 1× DEPC-treated PBS. Fixation was performed by suspending worms in 1 mL of fixation buffer [3.7% (vol/vol) formaldehyde in 1× DEPC-treated PBS] for 45 min rotating at room temperature. After fixation, worms were washed twice in 1 mL of 1× DEPC-treated PBS. Fixed animals were permeabilized overnight at 4 °C in 70% ethanol in DEPC-treated H_2O. Following permeabilization, worms were washed once in 1 mL of wash buffer [10% (vol/vol) formamide in 2× RNase-free SSC] then hybridized in 100 μL of hybridization buffer (0.2 g of dextran sulfate, 200 μL of 20× RNase-free SSC, 200 μL of deionized formamide, and 1.5 mL of DEPC-H_2O) with 1.25 μM probe. Worms were incubated at 30 °C overnight. These animals were washed in 1 mL of wash buffer for 30 min at room temperature, and then washed again in 1 mL wash buffer with 25 ng/mL DAPI counterstain for 30 min at room temperature. Animals were mounted for imaging on glass slides by using VECTASHIELD mounting media (Vector Laboratories) before epifluorescence or confocal microscopy.

ACKNOWLEDGMENTS. We thank L. Garwood for mapping *yp10* and *yp11*; T. Zucchero, L. Shtessel, L. Wu, J. Mitchell, and L. Leopold for technical assistance; J. Lieb for assistance with microarrays; and M. Tijsterman for strains. Some strains used in this work were provided by the *Caenorhabditis*

Genetics Center, which is funded by the National Institutes of Health (NIH) National Center for Research Resources. This research was supported by NIH Grant GM083048 (to S.A.), by National Institute of General Medical Sciences Grant K12GM000678 (to S.M.A), by a Cancer Research UK Programme Grant (to E.A.M.), an European Research Council starting grant (to E.A.M.), and by a Research Fellowship from Gonville and Caius College, Cambridge (to P.S.).

1. Fumagalli M, et al. (2012) Telomeric DNA damage is irreparable and causes persistent DNA-damage-response activation. *Nat Cell Biol* 14(4):355–365.
2. Sharpless NE, DePinho RA (2007) How stem cells age and why this makes us grow old. *Nat Rev Mol Cell Biol* 8(9):703–713.
3. Weismann A (1882) *Ueber die Dauer des Lebens* (G. Fischer, Jena, Germany).
4. Shay JW, Wright WE (2005) Senescence and immortalization: Role of telomeres and telomerase. *Carcinogenesis* 26(5):867–874.
5. Ahmed S, Hodgkin J (2000) MRT-2 checkpoint protein is required for germline immortality and telomere replication in C. elegans. *Nature* 403(6766):159–164.
6. Meier B, et al. (2006) trt-1 is the Caenorhabditis elegans catalytic subunit of telomerase. *PLoS Genet* 2(2):e18.
7. Hofmann ER, et al. (2002) Caenorhabditis elegans HUS-1 is a DNA damage checkpoint protein required for genome stability and EGL-1-mediated apoptosis. *Curr Biol* 12(22): 1908–1918.
8. Tijsterman M, May RC, Simmer F, Okihara KL, Plasterk RH (2004) Genes required for systemic RNA interference in Caenorhabditis elegans. *Curr Biol* 14(2):111–116.
9. Yabuta Y, et al. (2011) TDRD5 is required for retrotransposon silencing, chromatoid body assembly, and spermiogenesis in mice. *J Cell Biol* 192(5):781–795.
10. Han W, Sundaram P, Kenjale H, Grantham J, Timmons L (2008) The Caenorhabditis elegans rsd-2 and rsd-6 genes are required for chromosome functions during exposure to unfavorable environments. *Genetics* 178(4):1875–1893.
11. Zhang C, et al. (2012) The Caenorhabditis elegans RDE-10/RDE-11 complex regulates RNAi by promoting secondary siRNA amplification. *Curr Biol* 22(10):881–890.
12. Ashe A, et al. (2012) piRNAs can trigger a multigenerational epigenetic memory in the germline of C. elegans. *Cell* 150(1):88–99.
13. Frøkjaer-Jensen C, et al. (2008) Single-copy insertion of transgenes in Caenorhabditis elegans. *Nat Genet* 40(11):1375–1383.
14. Dernburg AF, Zalevsky J, Colaiácovo MP, Villeneuve AM (2000) Transgene-mediated cosuppression in the C. elegans germ line. *Genes Dev* 14(13):1578–1583.
15. Ketting RF, Plasterk RH (2000) A genetic link between co-suppression and RNA interference in C. elegans. *Nature* 404(6775):296–298.
16. Metzstein MM, Stanfield GM, Horvitz HR (1998) Genetics of programmed cell death in C. elegans: Past, present and future. *Trends Genet* 14(10):410–416.
17. Avgousti DC, Palani S, Sherman Y, Grishok A (2012) CSR-1 RNAi pathway positively regulates histone expression in C. elegans. *EMBO J* 31(19):3821–3832.
18. Claycomb JM, et al. (2009) The Argonaute CSR-1 and its 22G-RNA cofactors are required for holocentric chromosome segregation. *Cell* 139(1):123–134.
19. van Wolfswinkel JC, et al. (2009) CDE-1 affects chromosome segregation through uridylation of CSR-1-bound siRNAs. *Cell* 139(1):135–148.
20. Volpe TA, et al. (2002) Regulation of heterochromatic silencing and histone H3 lysine-9 methylation by RNAi. *Science* 297(5588):1833–1837.
21. Batista PJ, et al. (2008) PRG-1 and 21U-RNAs interact to form the piRNA complex required for fertility in C. elegans. *Mol Cell* 31(1):67–78.
22. Ruby JG, et al. (2006) Large-scale sequencing reveals 21U-RNAs and additional microRNAs and endogenous siRNAs in C. elegans. *Cell* 127(6):1193–1207.
23. Han T, et al. (2009) 26G endo-siRNAs regulate spermatogenic and zygotic gene expression in Caenorhabditis elegans. *Proc Natl Acad Sci USA* 106(44):18674–18679.
24. Conine CC, et al. (2010) Argonautes ALG-3 and ALG-4 are required for spermatogenesis-specific 26G-RNAs and thermotolerant sperm in Caenorhabditis elegans. *Proc Natl Acad Sci USA* 107(8):3588–3593.
25. Reinke V, Gil IS, Ward S, Kazmer K (2004) Genome-wide germline-enriched and sex-biased expression profiles in Caenorhabditis elegans. *Development* 131(2):311–323.
26. Conine CC, et al. (2013) Argonautes promote male fertility and provide a paternal memory of germline gene expression in C. elegans. *Cell* 155(7):1532–1544.
27. Katz DJ, Edwards TM, Reinke V, Kelly WG (2009) A C. elegans LSD1 demethylase contributes to germline immortality by reprogramming epigenetic memory. *Cell* 137(2):308–320.
28. Greer EL, et al. (2014) A histone methylation network regulates transgenerational epigenetic memory in C. elegans. *Cell Reports* 7(1):113–126.
29. Alvares SM, Mayberry GA, Joyner EY, Lakowski B, Ahmed S (2014) H3K4 demethylase activities repress proliferative and postmitotic aging. *Aging Cell* 13(2):245–253.
30. Patil VS, Kai T (2010) Repression of retroelements in Drosophila germline via piRNA pathway by the Tudor domain protein Tejas. *Curr Biol* 20(8):724–730.
31. Liu L, Qi H, Wang J, Lin H (2011) PAPI, a novel TUDOR-domain protein, complexes with AGO3, ME31B and TRAL in the nuage to silence transposition. *Development* 138(9):1863–1873.
32. Bagijn MP, et al. (2012) Function, targets, and evolution of Caenorhabditis elegans piRNAs. *Science* 337(6094):574–578.
33. Huang HY, et al. (2011) Tdrd1 acts as a molecular scaffold for Piwi proteins and piRNA targets in zebrafish. *EMBO J* 30(16):3298–3308.
34. Shoji M, et al. (2009) The TDRD9-MIWI2 complex is essential for piRNA-mediated retrotransposon silencing in the mouse male germline. *Dev Cell* 17(6):775–787.
35. Vasale JJ, et al. (2010) Sequential rounds of RNA-dependent RNA transcription drive endogenous small-RNA biogenesis in the ERGO-1/Argonaute pathway. *Proc Natl Acad Sci USA* 107(8):3582–3587.
36. Blanchard D, et al. (2011) On the nature of in vivo requirements for rde-4 in RNAi and developmental pathways in C. elegans. *RNA Biol* 8(3):458–467.
37. Gent JI, et al. (2010) Distinct phases of siRNA synthesis in an endogenous RNAi pathway in C. elegans soma. *Mol Cell* 37(5):679–689.
38. Kennedy S, Wang D, Ruvkun G (2004) A conserved siRNA-degrading RNase negatively regulates RNA interference in C. elegans. *Nature* 427(6975):645–649.
39. Simmer F, et al. (2002) Loss of the putative RNA-directed RNA polymerase RRF-3 makes C. elegans hypersensitive to RNAi. *Curr Biol* 12(15):1317–1319.
40. Sijen T, et al. (2001) On the role of RNA amplification in dsRNA-triggered gene silencing. *Cell* 107(4):465–476.
41. Tops BB, et al. (2005) RDE-2 interacts with MUT-7 to mediate RNA interference in Caenorhabditis elegans. *Nucleic Acids Res* 33(1):347–355.
42. Tabara H, et al. (1999) The rde-1 gene, RNA interference, and transposon silencing in C. elegans. *Cell* 99(2):123–132.
43. Buckley BA, et al. (2012) A nuclear Argonaute promotes multigenerational epigenetic inheritance and germline immortality. *Nature* 489(7416):447–451.
44. Simon M, et al. (2014) Reduced insulin/IGF-1 signaling restores germ cell immortality to caenorhabditis elegans Piwi mutants. *Cell Reports* 7(3):762–773.
45. Slotkin RK, Martienssen R (2007) Transposable elements and the epigenetic regulation of the genome. *Nat Rev Genet* 8(4):272–285.
46. Brenner S (1974) The genetics of Caenorhabditis elegans. *Genetics* 77(1):71–94.
47. Harris J, et al. (2006) Mutator phenotype of Caenorhabditis elegans DNA damage checkpoint mutants. *Genetics* 174(2):601–616.
48. Kamath RS, et al. (2003) Systematic functional analysis of the Caenorhabditis elegans genome using RNAi. *Nature* 421(6920):231–237.
49. Kamath RS, Martinez-Campos M, Zipperlen P, Fraser AG, Ahringer J (2001) Effectiveness of specific RNA-mediated interference through ingested double-stranded RNA in Caenorhabditis elegans. *Genome Biol* 2(1):RESEARCH0002.
50. Chomczynski P, Sacchi N (1987) Single-step method of RNA isolation by acid guanidinium thiocyanate-phenol-chloroform extraction. *Anal Biochem* 162(1):156–159.
51. Ikegami K, Egelhofer TA, Strome S, Lieb JD (2010) Caenorhabditis elegans chromosome arms are anchored to the nuclear membrane via discontinuous association with LEM-2. *Genome Biol* 11(12):R120.
52. Selzer RR, et al. (2005) Analysis of chromosome breakpoints in neuroblastoma at subkilobase resolution using fine-tiling oligonucleotide array CGH. *Genes Chromosomes Cancer* 44(3):305–319.
53. Davis MW, et al. (2005) Rapid single nucleotide polymorphism mapping in C. elegans. *BMC Genomics* 6:118.
54. Patterson GI, Padgett RW (2000) TGF beta-related pathways. Roles in Caenorhabditis elegans development. *Trends Genet* 16(1):27–33.